Autonomous Object Manipulation using a Soft Planar Grasping Manipulator

Robert K. Katzschmann, Andrew D. Marchese, and Daniela Rus*

July 7, 2015

Abstract

This paper presents the development of an autonomous motion planning algorithm for a soft planar grasping manipulator capable of grasp-and-place operations by encapsulation. The gripping end of the soft manipulator is fabricated without weakening seams using lost-wax casting instead of the commonly used multi-layer lamination process. The soft manipulation system can grasp randomly positioned objects within its reachable envelope and move them to a desired location without human intervention. The autonomous planning system leverages the compliance and continuum bending of the soft grasping manipulator to achieve repeatable grasps in the presence of uncertainty. Modeling uncertainties arise from a simplifying constant-curvature assumption, unrepresented manipulator dynamics, stick-slip friction, and non-linear fluidic control. These uncertainties are compensated by the inherent compliance of the soft gripper design and the motion planning strategy. Additionally, when fully actuated, the manipulator remains compliant allowing it to conform to un-modeled object geometries. A suite of experiments is presented that demonstrates the system's capabilities.

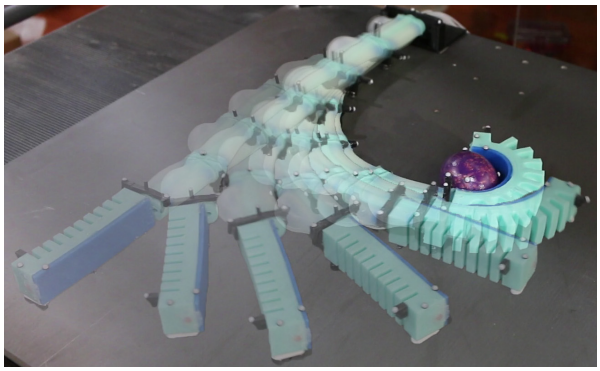

Figure 1: The soft manipulator is grasping a hollowed-out egg. The robot repeatably approached, grasped and moved this delicate object without breaking it.

1 Introduction

Soft robots exhibit continuum body motion, large scale deformation, high compliance and adjustable impedance compared to traditional rigid-bodied robots with high impedance Trivedi et al. [2008]. Such characteristics make this class of robots well-suited for highly dexterous tasks and interactions that require conformation to environmental uncertainty.

Our goal is to develop a soft planar fluid-powered gripper and a motion planning algorithm that leverages a soft morphology to robustly grasp, drag and place objects.

Our manipulator is highly compliant and its motion is not as precise as more traditional rigid-bodied robots. The control of its configuration is not only limited by the compliance of its low-pressure actuation, but also by its inherent elasticity. Despite the constraints on accurate positioning introduced by the softness of the arm, we can still robustly execute autonomous grasping tasks.

The fluid-powered gripper at the end of the arm can grasp an object through an open-loop controlled bending motion, even if the gripper is positioned relatively inaccurately in relation to the object to be grasped. The design of the gripper itself is inspired by work of Polygerinos et al. Polygerinos et al. [2013] The design is advantageous for grasping, because it exhibits high curvature, minimal radial expansion, and remains compliant during actuation. We can repeatably fabricate the gripper using a lost-wax casting process instead of the commonly used soft lithography technique, a multi-layer lamination process. Without weakening seams, the gripper is not prone to de-lamination under high deformations. By abandoning the need for a lamination process, arbitrary shaped internal channels can be achieved. The gripper was used as a manually actuated single finger with a bend sensor as part of a 3-fingered-hand in Homberg et al. [2015].

We attach the gripper to a multi-segment soft manipulator to enable autonomous grasp-and-place capabilities on a plane. Positional feedback is provided in real-time from a camera system. We present a planning algorithm that advances the arm through all necessary states of the grasp-and-place operation. A minimal strain, collision-free approach to the object of interest is found by posing the plan as a series of constrained nonlinear optimization problems. The system first plans concentric approach circles shrinking from the initial end-effector pose down to the object diameter. Next, the system searches

*Robert K. Katzschmann, Andrew D. Marchese, and Daniela Rus are with the Computer Science and Artificial Intelligence Laboratory, Massachusetts Institute of Technology, 32 Vassar St. Cambridge, MA 02139, USA, {rkk, andy, rus}@csail.mit.edu

for locally optimal manipulator configurations that constrain the end-effector to lie on these approach circles, so that the manipulator does not collide with the object. The manipulator is then moved between these plans using closed-loop trajectories. After successfully approaching the object, the gripper encapsulates it. We experimentally validate the system's ability to repeatably and autonomously grasp-and-place a randomly placed object.

1.1 Related Work

There are several examples of soft grippers described in recent literature, we will mainly focus on fluidic-based systems. Deimel and Brock Deimel and Brock [2013] developed a pneumatically actuated three-fingered hand made of reinforced silicone that is mounted to a hard robot and capable of grasping. More recently, they have developed an anthropomorphic soft pneumatic hand capable of dexterous grasps, which is not mounted to a robot, but instead just held by a humanDeimel and Brock [2014]. Ilievski et al. Ilievski et al. [2011] create through a soft-lithography fabrication a pneumatic starfish-like gripper composed of an array of silicone chambers and a PDMS membrane. The gripper is hanging on a string and grasps objects like an egg or a mouse in an open-loop controlled manner. Stokes et al. Stokes et al. [2014] use a soft elastomer quadrupedal robot to grasp objects in a hard-soft hybrid robotic platform. A puncture resistant soft pneumatic gripper is developed by Shepherd et al. in Shepherd et al. [2013]. An alternative to positive pressure actuated soft grippers is a robotic gripper that makes use of granular material jamming developed by Brown et al. and detailed in Brown et al. [2010]. The soft octopus-inspired arms developed in Calisti et al. [2010] and Calisti et al. [2011] are not fluidic powered, but instead use cables to pull rigid fixtures embedded within an elastomer body. The arms were capable of grasping objects like pens or screws. A soft robotic tentacle developed in Martinez et al. [2013] was able to hold a flower and a horseshoe-shaped object. The closest related soft pneumatic actuator design to our current work is the fast Pneu-net designs by Mosadegh et al. detailed in Mosadegh et al. [2014] and by Polygerinos et al. detailed in Polygerinos et al. [2013]. These finger-like actuators deform with minimal volume change and can bend to high curvatures. None of the above described grippers were controlled autonomously to perform their tasks and accordingly no statement on repeatability of the autonomous execution was given.

Cho et al. Cho et al. [2009] review several manufacturing processes for soft biomimetic robots. The vast majority of soft elastomer robots rely on the processes of soft lithography Xia and Whitesides [1998] and/or shape deposition manufacturing Cham et al. [2002]. Especially noteworthy is the use of lost-wax fabrication for jammable skin chambers, which get vacuumed to stiffen up Steltz et al. [2009]. The gripper presented here also uses a lost-wax molding technique, but with a different type of actuation in mind: the obtained cavity structures are inflated to cause the gripper to bend.

More recently, Marchese et al. demonstrated closed-loop position control of multi-segment soft planar fluidic elastomer manipulators in free space Marchese et al. [2014b] and in confined spaces Marchese et al. [2014a]. Positioning is achieved using forward and inverse kinematic models and real-time camera measurements. The manipulator curvatures are controlled in real-time using a curvature-volume cascaded control law. The work presented in this paper builds on top of this system and expands its capabilities. The previous version was only suitable for contactless motions in space, that would be suitable for mere inspection. The work presented here is capable of autonomous object manipulation on a plane. Furthermore, this work shows that combining two different soft actuator types can leverage the strength of each and together achieve a more complicated task of manipulating objects. The control of the arm is improved from the previous version by using a more robust vision tracking approach. Previously, there were only single markers along the arm, which worked for a limited motion range, but was prone to fail if the markers go out of sight or another object is introduced to the environment. Also, many trial runs were needed to arrive at the various final positions in the maze.

1.2 Contributions

This work differs from the previous work in that we do not attach a novel soft gripper to a hard arm nor do we move the gripper around manually, but we rather take on the challenge of grasping-and-placing objects with a seven degrees of freedom planar arm made entirely from soft rubber. We provide in this work the following contribution to soft robotics:

- A soft manipulator consisting of a multi-segment arm with a gripper to enable fully compliant planar grasping.
- A planning algorithm to grasp-and-place randomly positioned objects on a planar surface using a 7 DOF soft manipulator.
- Repeatable successful grasping demonstrations with a physical prototype and an experimental characterization of the uncertainty regions that can be tolerated by the soft gripper.
- Demonstrate that soft robots do neither require force sensing nor accurate positioning to allow for proper manipulation of delicate objects.

2 System Overview

The aggregate system is shown in Figure 2 and consists of a manipulator, a gripper, an object, a tracking system, control computers, a fluidic drive array and a rigid frame. The planar six segment soft rubber manipulator consists of twelve distributed elastomer actuators. This manipulator moves with minimal friction on a level plane. A soft rubber gripper is fixed to the tip of the manipulator. An object is randomly placed within the reachable envelop of the manipulator. A motion capture system provides real-time measurements of marked

points both along the inextensible back of the manipulator and on top of the object. The grasp motion planning algorithm as well as the curvature controller run on the control computers and take the tracking information as input. The curvature controller then provides continuous closed-loop adjustment of the fluidic drive cylinder array. The cylinder array directly actuates the manipulator and gripper. A rigid frame holds all the subsystems together providing reliable and consistent hardware experiments.

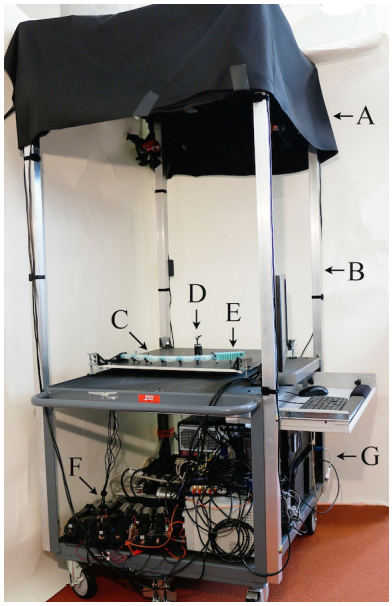

Figure 2: System Overview. The system is composed of a motion capture system (A), rigid frame (B), soft six segment planar manipulator (C), an object within the grasp envelope (D), a soft gripper fixed to the manipulator (E), a fluidic drive cylinder array to control actuation (F), and computers for real-time processing and control (G).

3 Soft Grasping Manipulator

We describe briefly the design, fabrication and functionality of the soft grasping manipulator. Further details on the design and fabrication can be found in Marchese et al. [2015].

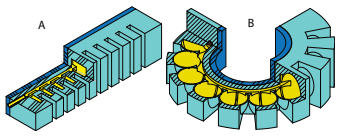

Figure 3: The pleated channel designs. (**A**) depicts the segment in an unactuated state and (**B**) shows the segment in an actuated and therefore bent state. The expansion of the pressurized channels are schematically represented.

3.1 Pleated Channel Design for the Gripper

The pleated channel design consists of evenly spaced ribs shown in *cyan* with embedded hollow sections shown in *yellow*. Cut views of the un-actuated and actuated states are shown in Figure 3. This design approach draws inspiration for its pleats from the soft pneumatic gloves developed by Polygerinos et al. Polygerinos et al. [2013] and its homogeneous body design is inspired from the tail design of a soft robotic fish developed by Katzschmann et al. Katzschmann et al. [2014]. This design is advantageous for grasping because it exhibits high curvature, minimal radial expansion, and remains compliant during actuation Marchese et al. [2015]. The hollow ribs within the segment's pleats are connected by a center channel and are accessible through a front inlet. Under fluidic pressurization of the interior channel, an individual pleat allows for a ballon-like expansion of the thin exterior skin along the axial direction. Similar to the uniform channel design, a stiffer silicone layer shown in *blue* serves as an almost inextensible constraint layer. The sum of the ballon-like expanding motions leads to bending of the less extensible center constraint layer to form a grasp. The pleated design is capable of unidirectional bending up to extreme curvatures. Using a lost-wax casting approach, we are not limited in defining the geometry of the segment's fluidic channels. Using this approach, the *cyan* portion of the pleated gripper can be cured in a single step, avoiding any weakening seams due to lamination. Those seams are prone to rupture and manufacturing inconsistencies.

3.2 Lost Wax Fabrication for Fluidic Elastomer Actuators

Existing soft fluidic manipulators are produced through a multi-step lamination process, which results in weakening seams that can easily delaminate. This limits their range of applications and lifetime. This is why we propose the application of lost-wax casting to the fabrication of soft fluidic actuators like a gripper. The actuated cavities of the soft gripper are achieved by using a wax core, pourable silicone rubber and 3D printed molds. The complete fabrication process for the soft gripper consists of eight steps that are depicted in Figure 4. The tools and equipment used are listed in Table 1 and are referred to by superscripts.

In step (A), harder silicone rubber[6] is poured into a mold, which contains a printed model of the wax core. In preparation for step (B), the model is removed and the rubber mold is left inside the outer mold. A rigid rod is used as a supportive inlay inside the wax core. The rod is laid into the cavity of the rubber mold, supported on both ends by the outer mold. This ensures that the wax core does not break when removed from the rubber mold. The bees-wax[7] is heated up until it becomes fully liquefied. The assembly of rubber mold and outer mold is then heated up for a few minutes to the same temperature as the wax. Using a syringe, the liquid wax is injected into the assembly. Within a few minutes, the injected wax will start to solidify and significantly shrink in volume; this is counter-

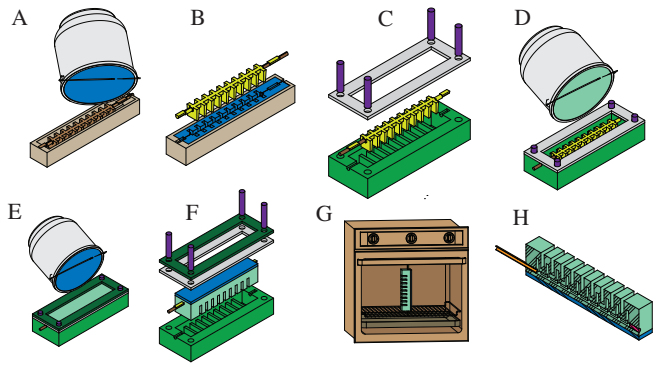

Figure 4: Gripper fabrication process. (**A**) Pour and cure a rubber mold, (**B**) pour wax core with embedded supportive rod, (**C**) combine bottom mold, top mold and wax core using pins, (**D**) pour rubber into assembled mold, (**E**) pour stiffer rubber on top of the cured gripper to form a constraint layer, (**F**) remove cured gripper from mold, (**G**) using an oven melt out wax core from the gripper, and (**H**) add silicone tubing and plug using silicone sealant.

acted by injecting more hot wax into the solidifying wax core during cool down. In step (B), the wax core is first allowed to completely cool down, then it is released from the mold. In step (C), the cooled down wax core is assembled together with the bottom mold, which defines the pleated structure of the gripper. The mold assembly is aligned with a top mold using pins. This top mold provides for additional volume to cover the wax core. In step (D), low elastic modulus rubber[1] is mixed, degassed in a vacuum[2], and poured to form the gripper and allowed to cure. In step (E), stiffer rubber[3] is poured on top of the cured gripper to form a constraint layer. In step (F), the cured gripper is removed from the mold. In step (G), most of the wax core is melted out by placing the gripper into an oven in an upright position. After this, remaining wax residues are cooked out in a boiling water bath. Finally, in step (H) a silicone tube[5] and a piece of silicone cord[8] get covered with silicone sealant[4] and are inserted into the front and back holes respectively.

Table 1: Commercially Available Tools and Equipment

#	Product Name	Company
1	Ecoflex 0030	Smooth-On
2	AL Cube	Abbess Instruments and Systems, Inc.
3	Mold Star 15	Smooth-On
4	Silicone Sealant 732	Dow Corning Corp
5	PN 51845K53	McMaster
6	Mold Star 30	Smooth-On
7	Beeswax	Jacquard
8	PN 9808K21	McMaster

3.3 Multi-segment Arm with Gripper

The design for our arm consisting of soft cylindrical segments was described in Marchese et al. [2014a]. Each cylindrical segment can only be actuated up to a bend angle of less than 60°, therefore several segments have to be combined together to allow the arm to reach a large enough workspace to perform proper manipulation tasks on a plane. Our cylindrical design with its hollow channel in the center has enough space to accomodate for pneumatic tubes to connect to all six cylindrical segments and additionally to the pleated gripper, which is attached to the tip. The pleated gripper has to be appropriately sized, just big enough to allow for proper manipulation without exceeding the payload capacity of the soft arm.

The independent actuation of the unidirectional gripper and each bidirectional arm segment is achieved through an array of custom fluidic drive cylinders. Those cylinders are driven by a linear actuator and controlled through a motor controller, which takes its command signals from a higher-level curvature controller. The modeling and design of these are described in Marchese et al. [2014b].

4 Planning and Control

4.1 Existing Procedures

The forward kinematics algorithm `forwKin()`, which we employ in this work, assumes piece-wise constant curvature according to Webster and Jones [2010]. This algorithm was experimentally validated for the soft planar arm in Marchese et al. [2014b]. In order to uniquely fit a configuration representation to measured endpoint data in real-time, we use a previously developed single segment inverse kinematics algorithm Marchese et al. [2014b] and refer to it in this work as `singSegInvKin()`. The inputs to this block are the start and endpoint measurements in $\mathbb{R}^2$: $\mathbf{E}_n \ \forall n = 1..N$, where N is the number of segments composing the arm. The outputs from this block are the representations of the measured manipulator configuration: $\boldsymbol{\kappa}_{\text{meas}}$ and $\mathbf{L}_{\text{meas}}$. This work expands on the previously developed cascaded closed-loop curvature controller, whose input is target curvatures $\boldsymbol{\kappa}_{\text{target}}$ and whose output is the controlled adjustment of a fluidic drive cylinder array to resolve the error between $\boldsymbol{\kappa}_{\text{target}}$ and $\boldsymbol{\kappa}_{\text{meas}}$. In this work we refer to it as the `curvatureController()`.

The planning algorithm presented in Marchese et al. [2014a] was developed to plan the motion of a soft arm without gripper through a confined environment. The optimization constraints and state machine setup in that work is significantly different and not applicable to the grasping shown here. Therefore, a new planner is presented in the following section.

4.2 Grasp-and-Place Planner

The robotic manipulation system is capable of autonomously performing grasp-and-place operations. A state flow diagram describing its sensing, planning and executions states is given in Fig. 5. A motion tracker constantly captures the position

of the object and passes it along to a routine, which checks for the object to settle. After it has settled, the grasp object planner receives the coordinates and radius of the settled object and together with the current curvature values of the arm and gripper, it solves a series of constrained nonlinear optimization problems to generate end-effector poses approaching the object. Those end-effector poses are essentially waypoints for an optimized path the robot arm should take to get to the final position without the risk of pushing away the object before the gripper arrives there. Forcing the arm controller to follow those intermediate waypoints ensures that the arm moves to the object while its nullspace maintains a convex shape, bending away from the object. Furthermore, it allows the arm to move in smaller portions, decreasing the risk of large overshoots due to slip-stick friction between the roller supports and the ground. This planner is described in more detail in Section 4.3.

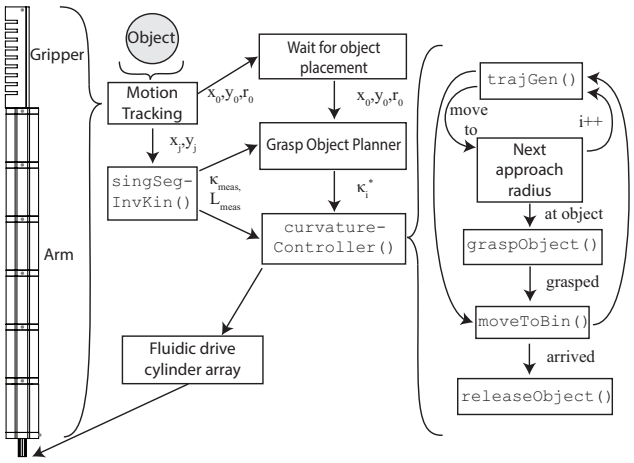

Figure 5: State flow diagram of the grasp-and-place planner developed for the autonomous grasp-and-place operation of the manipulator. This diagram describes essentially the flow of information from the motion tracking system to the discrete hardware.

The grasp object planner passes the approach configurations $\boldsymbol{\kappa}_i^*$ of the arm to the `curvatureController()` for execution in real-time. The controller receives measured curvatures $\boldsymbol{\kappa}_{meas}$ and lengths $\boldsymbol{L}_{meas}$ at an update rate of 100 Hz from the recursively called `singSegInvKin()` and uses these to successively control the arm to every intermediate configuration $\boldsymbol{\kappa}_i^*$. During the arm initialization, the new curvature controller performs a pre-pressurization of both lateral channels. This is only done for the two segments closest to the root of the arm in order to stiffen them and shorten their response time constant. To allow for smoother transitions between each configuration $\boldsymbol{\kappa}_i^*$, we also added a trajectory generation procedure `trajGen()` to the new curvature controller. It generates in real-time for each individual degree-of-freedom velocity profiles with acceleration and velocity constraints. These profiles allow real-time interpolation between the approach configurations of the arm and avoid overshooting at the next target configuration. When the arm has arrived at the object, the curvature controller initiates `graspObject()`. After encapsulating the object, `moveToBin()` requests `trajGen()` for another trajectory from the current pose to a pre-defined bin location. After the manipulator has arrived at the bin location, the procedure `releaseObject()` causes the gripper to open and release the object.

4.3 Grasp Planner

A fundamental component of the grasp-and-place planner is the system's ability to plan a feasible approach motion to the object. That is, given the location (x_o, y_o) and radius r_o of a round object as well as the manipulator's current configuration $\boldsymbol{\kappa}_{\text{meas}}$, we determine a series of locally optimal manipulator configurations $\boldsymbol{\kappa}_i^* \ \forall i = 1..numMoves$ that will, if sequentially achieved, bring the manipulator gradually closer to the object while any part of the arm is not touching the object. We refer to these as approach configurations. The process for determining these approach configurations is detailed in the `planGrasp()` procedure within the Grasp Object Planner, see Algorithm 1. The planner is visualized in Figure 6. In short, we define a series of approach radii $r_{a_i} \ \forall i = 1..numMoves$ that define concentric circles shrinking from the manipulator's starting tip pose towards the center of the object. Given actuator limits, we then search for a series of feasible manipulator configurations $\boldsymbol{\kappa}_i^*$ that will place the robot's end-effector on these circles, parameterized by r_a and ϕ, while minimizing manipulator deformation.

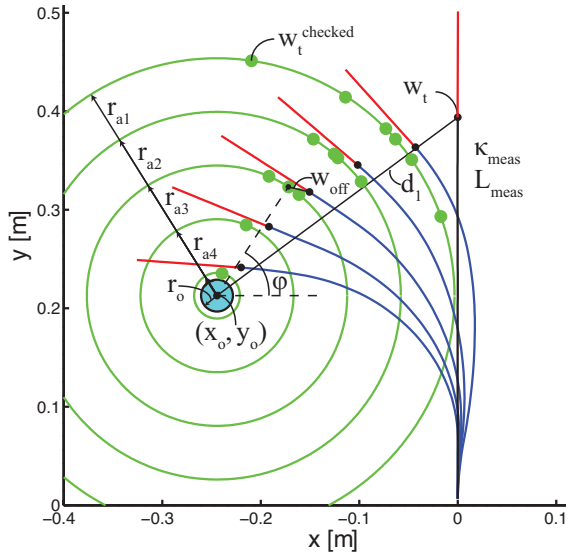

Figure 6: Grasp object planner visualization. Concentric approach circles are shown in *green* and are centered about the object shown in *cyan*. The locally optimal approach configurations are shown in *blue* and the gripper is shown in *red*. The initially measured manipulator configuration is shown in black.

The procedure first determines the manipulator's current tip pose $\mathbf{w}_t$ and the Euclidean distance d_1 between the tip and the object's center. Next, considering the object's radius r_o and

Algorithm 1: Grasp object planner

Input: $\boldsymbol{\kappa}_{\text{meas}}, \mathbf{L}_{\text{meas}} \leftarrow$ measured arm configuration
$\boldsymbol{\kappa}_{\text{off}} \leftarrow$ bias configuration offset at start
$g_{\text{off}} \leftarrow$ gripper offset normal to end-effector
$x_o, y_o, r_o \leftarrow$ object center coordinates and radius
$N \leftarrow$ number of manipulator segments

Procedure `planGrasp()`

$\mathbf{w}_t \leftarrow$ `forwKin` $(\boldsymbol{\kappa}_{\text{meas}}, \mathbf{L}_{\text{meas}}, N, L_N)$.
$d_1 \leftarrow \| [x_o, y_o]^{\mathrm{T}} - \mathbf{w}_t \|$.
$d_2 \leftarrow d_1 - r_o - g_{\text{off}}$.
$numMoves \leftarrow \lfloor \frac{d_2}{\Delta d} \rfloor$.
$i = 0$.
repeat
  $i = i + 1$
  $r_{a_i} \leftarrow d_1 - i \frac{d_2}{numMoves}$.
  $\boldsymbol{\kappa}_i^* \leftarrow$ `findOptimalConfig` (r_{a_i})
until $i = numMoves$
return $\boldsymbol{\kappa}_i^* \quad \forall i = 1..numMoves$

Procedure `findOptimalConfig` (r_a)

$$\boldsymbol{\kappa}^* \leftarrow \min_{\boldsymbol{\phi}, \boldsymbol{\kappa}} \ \mathbf{R} \left(\boldsymbol{\kappa} - \boldsymbol{\kappa}_{\text{off}}\right)^2.$$

subject to

$$\mathbf{w}_t \leftarrow \begin{bmatrix} x_o + r\cos\phi \\ y_o + r\sin\phi \\ \phi + \frac{\pi}{2} \end{bmatrix}.$$

$$\mathbf{f} \leftarrow \texttt{forwKin}\,(\boldsymbol{\kappa}, \mathbf{L}, N, L_N).$$

$$\mathbf{w}_t - \mathbf{w}_{\text{off}}(r_o, \phi) - \mathbf{f} = \mathbf{0}.$$

$$\kappa_n^{\min} \le \kappa_n \le \kappa_n^{\max} \quad \forall n = 1..N.$$

return $\boldsymbol{\kappa}^*$

Procedure `forwKin` $(\boldsymbol{\kappa}, \mathbf{L}, i, s)$

Input: $\boldsymbol{\kappa}$, $\mathbf{L}$, i the segment of interest index, s the arc length along the indexed segment
if $i = 0$ **then**
  $\theta_i(0) \leftarrow \theta_0(0)$.
  $x_i(0) \leftarrow 0$.
  $y_i(0) \leftarrow 0$.
else
  $[x_i(0), y_i(0), \theta_i(0)] \leftarrow$ `forwKin` $(\boldsymbol{\kappa}, \mathbf{L}, i-1, L_{i-1})$.
end
$\theta \leftarrow \theta_i(0) + k_i s$.
$x \leftarrow x_i(0) + \frac{\sin\theta}{k_i} - \frac{\sin\theta_i(0)}{k_i}$.
$y \leftarrow y_i(0) - \frac{\cos\theta}{k_i} + \frac{\cos\theta_i(0)}{k_i}$.
return $[x, y, \theta]^{\mathrm{T}}$ *or* $[x, y]^{\mathrm{T}}$

the gripper normal offset $\mathbf{g}_{\text{off}}$, the minimal tip transit distance d_2 is calculated. $\mathbf{g}_{\text{off}}$ is the component of the end effector offset $\mathbf{w}_{\text{off}}$, which is normal to the end effector orientation. Also, the number of approach configurations $numMoves$ is determined as $\lfloor \frac{d_2}{\Delta d} \rfloor$, where Δd is an allowable incremental distance. Using these parameters, approach radii r_a are iteratively calculated and their corresponding locally optimal configurations are found using the `findOptimalConfig(`r_a`)` procedure. This process is posed as a nonlinear optimization. Here, the objective function represents the summation of independently weighted manipulator curvatures and the constraints force the manipulator's tip to lie on and to be tangent to the approach circle. This process leverages the arm's forward kinematics `forwKin()` defined in Marchese et al. [2014b] and reproduced in Algorithm 1 for convenience.

5 Experimental Results

5.1 Grasping Delicate Objects

The soft manipulator can pick up hollowed-out eggs and other delicate objects without breaking them. Figure 1 shows how the manipulator approaches and grasps an egg. Delicate objects can be manipulated without requiring a shape or a force sensor within its structure, since the compliant gripper body conforms to the object. Rigid-bodied grippers usually rely on force sensing or another type of sensory feedback to avoid damage caused to the object.

5.2 Repeated Grasp Experiments

We performed 25 experimental grasp-and-place trials at various positions to demonstrate the capabilities and repeatability of our system. The results of all the trials are shown in Figure 8. One representative approach, grasp, and retract move is shown in Figure 9. In 23 of 25 experimental trials, the manipulator successfully achieved the task of grasping an object and bringing it to a bin location shown in red. The object was placed five times on each of the five points marked on the board. The markers only serve as a reference point for the user to place the object roughly at the same point at every repetition. The user's placing accuracy is not important to the algorithm, the tracking system newly registers every single time the position of the placed object. The five points were chosen to approximately represent the major portion of the manipulator's reachable workspace. As long as the root of the gripper stops so that the object is located within the capture region, the gripper will pick it up through its sweeping closing motion. The capture region is shown in grey in Figure 7. When the arm reaches the red bin location, it drops the object.

The unsuccessful trials happened due to stick-slip friction between the roller bearings and the table surface. Our kinematic modeling does not account for this non-linear behavior, which acts as a disturbance and can lead to failure to arrive at the next waypoint. To be more specific, in one of the trials, the robot slowed down too much before it almost reached its next waypoint and because of friction the arm got to a full

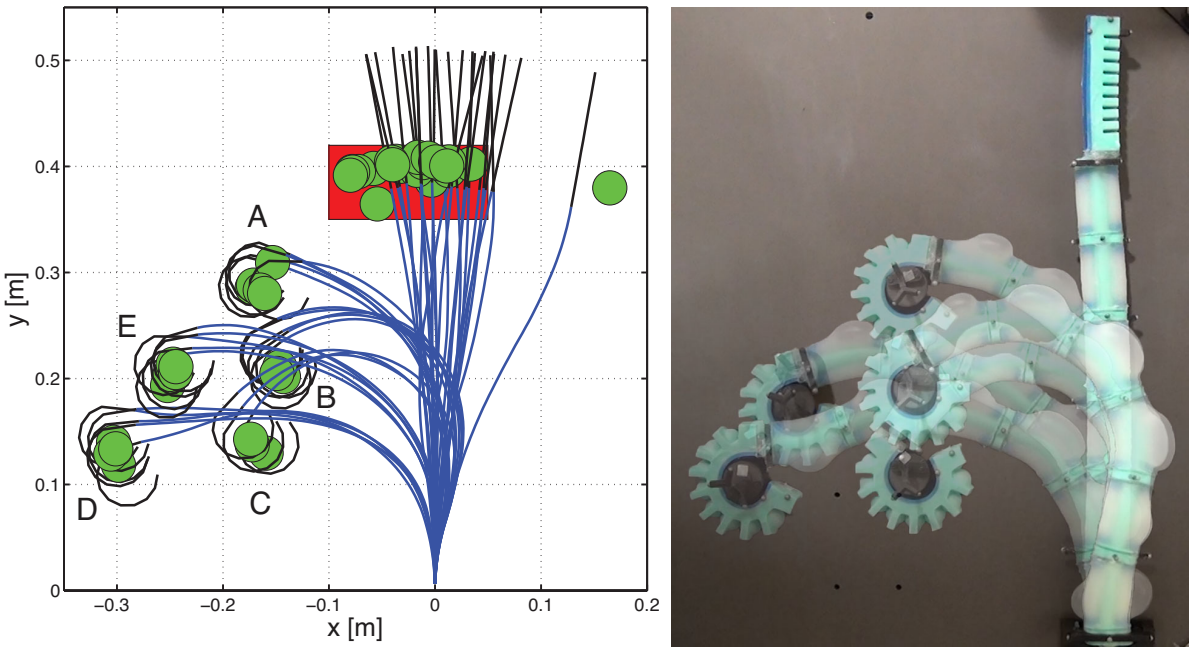

Figure 8: Complete set of experimental grasp-and-place trials. In these experiments, the arm moves from an initial straightened configuration to grasp a round object placed in one of five locations (A-E). The arm then returns the object to a bin location shown in red. For each trial, a seven degrees of freedom manipulator representation is generated at both the *grasped* and *released* state using experimental data and is shown in blue. The corresponding 1 degree-of-freedom end-effector representation is shown in black. The round object's measured position at each state is shown in green. Right: Overlaid photographs of the manipulator grasping an object placed at each of the five locations.

stop. The proportional gain of the curvature controller was not able to compensate for that small positional delta and since the relatively low saturation level of the integrator portion of the controller was saturated, the arm did not move to the next waypoint pose. It is to note, that the saturation level for the integrator is defined by a safety limit on the maximal inflation of the robotic arm. In the other unsuccesful trial, the stick-slip friction also caused the arm to halt before a waypoint. The controller built up enough forcing due to inflation, so that the arm slipped over the close waypoint without having all of its single arm segment curvature within an acceptable epsilon. The controller then tried to swing back to fulfill the missed waypoint, missed it again and that finally caused the whole arm to oscillate back-and-forth and eventually push the object off the table. In one of the other trials, the grasp and return was successfully performed, but a small overshoot over the final bin location at the end of the return caused the arm to drop off the table, which could have been avoided if the table would have not been too small towards the right. This outlier is shown in Figure 8. Overall, the experiments show that the system was repeatably able to autonomously locate a randomly placed object within its workspace, plan the arm motions, and perform the task of grasping and placing the object.

5.3 Experimental Insights and Limitations

The system can drag payloads of less than 40 g, higher payloads cause the cylindrical arm segments to stall and possibly lift off the table without moving the payload. There is a trade-off between the reachable workspace and the maximum payload. As the length of the arm increases, more workspace can be reached while less payload can be manipulated. Most of the payload capability is already used up by the attached gripper itself. A smaller gripper would allow for larger payloads to get picked up, but consequently only smaller objects can be grasped. The workspace of the manipulator is limited to the top and left by the maximal extension length of the arm, and to the bottom by the maximum bending curvature, which the arm can achieve without over-actuating a single segment. Objects were only grasped within the left quadrant of the arm, because of the gripper orientation and an upright initial starting pose.

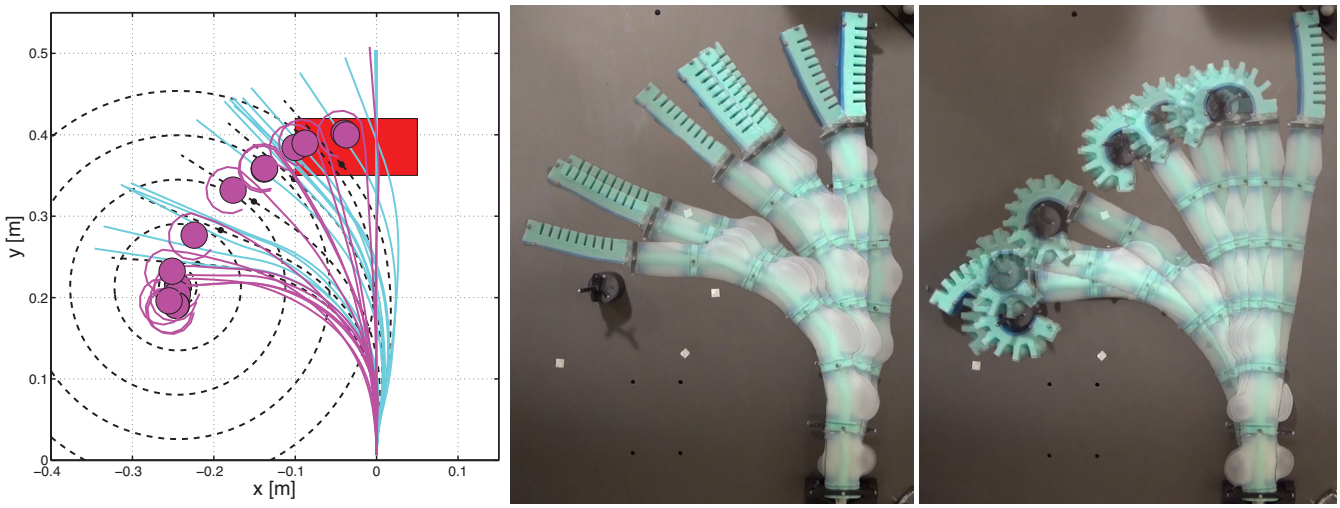

Figure 9: Left: A time series representation of an experimental grasp-and-place trial for an object located at point E. Here, the locally optimal planned manipulator configurations as well as planned sequential approach circles are shown as black dotted curves. The arm and gripper are shown in their experimentally determined configuration representations at 1 second intervals. The cyan configurations represent the manipulator prior to grasping the object, that is moving from its initial configuration to the object's location. The magenta configurations represent the manipulator after grasping the object, that is moving from the object's location back to the bin location shown in red. Right: A photograph of the arm moving from its initial pose to the object and from the object to the release location, respectively.

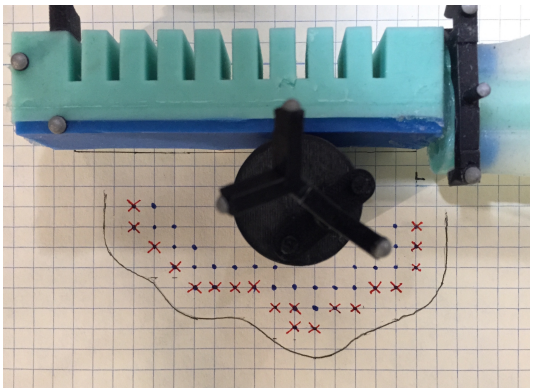

Figure 7: Experimental characterization of the gripper's capture region: the allowable positioning uncertainty is determined through repeated placements of the center of a cylindrical object at different points on a grid relative to the gripper. Blue dots indicate all object center positions for which a grasp could be performed successfully, red crosses show the positions where a grasp failed. The grey line outlines an area for the object to be positioned within so the gripper can grasp it. The evaluation of the capture region was performed similarly to a method described in Dogar and Srinivasa [2010].

6 Conclusion

This work introduced a new manufacturing approach for a soft manipulator and demonstrated its capabilities through autonomously grasping-and-placing a randomly positioned object. To produce the complete soft manipulator used, an entirely soft gripper was designed and fabricated and then combined with a previously developed soft robotic arm. It was then shown that a minimal strain and collision-free approach to an object of interest can be achieved by posing the grasp motion plan as a series of constrained nonlinear optimization problems.

The fabrication approach presented has potential to generalize beyond just the fabrication of a gripper. The new approach is advantageous because it allows for arbitrary designs of internal fluidic cavities and the casting of a homogeneous soft segment. It removes the need for laminating several separately casted parts together. Such a homogeneous soft segment is less prone to rupture and to manufacturing inconsistencies, and would therefore allow for better robot performance.

The results presented in this paper suggest that despite their extreme compliance, soft robots are capable of repeatable object manipulation while simultaneously providing inherently safe interactions with their environment. The manipulator is suitable to perform delicate tasks with low payloads, for example grasping objects that should not be squeezed and/or should not break during manipulation. We demonstrated the ability of an entirely soft manipulator to autonomously grasp an object, which leads to many potential applications. In a manufacturing setting, this could resemble a soft robot executing tasks requiring high dexterity when handling delicate objects. In a human-centric environment, soft arm grasping manipulation may enable soft robots to interact safely with humans. Furthermore, in a surgical setting, highly compliant soft robots with grippers may assist with operations in sensitive environments during tasks where no high level of precision is required.

ACKNOWLEDGMENTS

This research was conducted in the Distributed Robotics Laboratory at MIT with support from the National Science Foundation, grant numbers NSF 1117178, NSF IIS1226883 and NSF CCF1138967, and National Science Foundation Graduate Research Fellowship Program, primary award number 1122374. We are grateful for this support.

References

Eric Brown, Nicholas Rodenberg, John Amend, Annan Mozeika, Erik Steltz, Mitchell R Zakin, Hod Lipson, and Heinrich M Jaeger. Universal robotic gripper based on the jamming of granular material. *Proceedings of the National Academy of Sciences*, 107(44):18809–18814, 2010.

M Calisti, A Arienti, ME Giannaccini, M Follador, M Giorelli, M Cianchetti, B Mazzolai, C Laschi, and P Dario. Study and fabrication of bioinspired octopus arm mockups tested on a multipurpose platform. In *Biomedical Robotics and Biomechatronics (BioRob), 2010 3rd IEEE RAS and EMBS International Conference on*, pages 461–466. IEEE, 2010.

M Calisti, M Giorelli, G Levy, B Mazzolai, B Hochner, C Laschi, and P Dario. An octopus-bioinspired solution to movement and manipulation for soft robots. *Bioinspiration & biomimetics*, 6(3):036002, 2011.

Jorge G Cham, Sean A Bailey, Jonathan E Clark, Robert J Full, and Mark R Cutkosky. Fast and robust: Hexapedal robots via shape deposition manufacturing. *The International Journal of Robotics Research*, 21(10-11):869–882, 2002.

Kyu-Jin Cho, Je-Sung Koh, Sangwoo Kim, Won-Shik Chu, Yongtaek Hong, and Sung-Hoon Ahn. Review of manufacturing processes for soft biomimetic robots. *International Journal of Precision Engineering and Manufacturing*, 10 (3):171–181, 2009.

Raphael Deimel and Oliver Brock. A compliant hand based on a novel pneumatic actuator. In *Robotics and Automation (ICRA), 2013 IEEE International Conference on*, pages 2047–2053. IEEE, 2013.

Raphael Deimel and Oliver Brock. A novel type of compliant, underactuated robotic hand for dexterous grasping. In *Robotics: Science and Systems*, 2014.

M.R. Dogar and S.S. Srinivasa. Push-grasping with dexterous hands: Mechanics and a method. In *Intelligent Robots and Systems (IROS), 2010 IEEE/RSJ International Conference on*, pages 2123–2130, Oct 2010. doi: 10.1109/IROS.2010.5652970.

Bianca Homberg, Robert K Katzschmann, Mehmet Dogar, and Daniela Rus. Haptic Identification of Objects using a Modular Soft Robotic Gripper. In *Intelligent Robots and Systems (IROS), 2015 IEEE/RSJ International Conference on*, 2015.

Filip Ilievski, Aaron D Mazzeo, Robert F Shepherd, Xin Chen, and George M Whitesides. Soft robotics for chemists. *Angewandte Chemie*, 123(8):1930–1935, 2011.

Robert K Katzschmann, Andrew D Marchese, and Daniela Rus. Hydraulic Autonomous Soft Robotic Fish for 3D Swimming. In *2014 International Symposium on Experimental Robotics (ISER 2014)*, number 1122374, Marrakech, Morocco, 2014.

Andrew D Marchese, Robert K Katzschmann, and Daniela Rus. Whole Arm Planning for a Soft and Highly Compliant 2D Robotic Manipulator. In *Intelligent Robots and Systems (IROS), 2014 IEEE/RSJ International Conference on*. IEEE, 2014a.

Andrew D Marchese, Konrad Komorowski, Cagdas D Onal, and Daniela Rus. Design and control of a soft and continuously deformable 2d robotic manipulation system. In *Accepted for publication in: Robotics and Automation (ICRA), 2014 IEEE International Conference on*. IEEE, 2014b.

Andrew D. Marchese, Robert K. Katzschmann, and Daniela Rus. A Recipe for Soft Fluidic Elastomer Robots. *Soft Robotics*, 2(1):7–25, 2015. ISSN 2169-5172. doi: 10.1089/soro.2014.0022. URL http://online.liebertpub.com/doi/10.1089/soro.2014.0022.

Ramses V Martinez, Jamie L Branch, Carina R Fish, Lihua Jin, Robert F Shepherd, Rui Nunes, Zhigang Suo, and George M Whitesides. Robotic tentacles with three-dimensional mobility based on flexible elastomers. *Advanced Materials*, 25 (2):205–212, 2013.

Bobak Mosadegh, Panagiotis Polygerinos, Christoph Keplinger, Sophia Wennstedt, Robert F Shepherd, Unmukt Gupta, Jongmin Shim, Katia Bertoldi, Conor J Walsh, and George M Whitesides. Pneumatic networks for soft robotics that actuate rapidly. *Advanced Functional Materials*, 24 (15):2163–2170, 2014.

Panagiotis Polygerinos, Stacey Lyne, Zheng Wang, Luis Fernando Nicolini, Bobak Mosadegh, George M. Whitesides, and Conor J. Walsh. Towards a soft pneumatic glove for hand rehabilitation. In *Intelligent Robots and Systems (IROS), 2013 IEEE/RSJ International Conference on*, pages 1512–1517. Ieee, November 2013. ISBN 978-1-4673-6358-7. doi: 10.1109/IROS.2013.6696549.

Robert F Shepherd, Adam A Stokes, Rui Nunes, and George M Whitesides. Soft machines that are resistant to puncture and that self seal. *Advanced Materials*, 25(46): 6709–6713, 2013.

Erik Steltz, Annan Mozeika, Nick Rodenberg, Eric Brown, and Heinrich M Jaeger. JSEL: Jamming Skin Enabled Locomotion. In *Intelligent Robots and Systems, 2009. IROS 2009. IEEE/RSJ International Conference on*, pages 5672–5677. IEEE, October 2009. doi: 10.1109/IROS.2009.5354790.

Adam A Stokes, Robert F Shepherd, Stephen A Morin, Filip Ilievski, and George M Whitesides. A hybrid combining hard and soft robots. *Soft Robotics*, 1(1):70–74, 2014.

Deepak Trivedi, Christopher D Rahn, William M Kier, and Ian D Walker. Soft robotics: Biological inspiration, state of the art, and future research. *Applied Bionics and Biomechanics*, 5(3):99–117, 2008.

Robert J Webster and Bryan A Jones. Design and kinematic modeling of constant curvature continuum robots: A review. *The International Journal of Robotics Research*, 29 (13):1661–1683, 2010.

Younan Xia and George M Whitesides. Soft lithography. *Annual review of materials science*, 28(1):153–184, 1998.